Journal Pre-proof

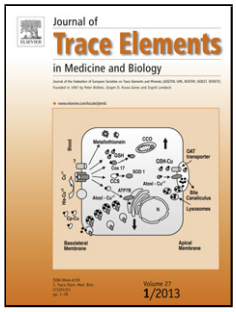

Fluoride Induced Down-regulation of IKBKG Gene Expression Inhibits Hepatocytes Senescence

Wu C.X., Mao C.Y., Deng J., Zhang T., Zhao Y., Guan Z.Z., Hu X.X., Qi X.L.

PII: S0946-672X(21)00186-3

DOI: https://doi.org/10.1016/j.jtemb.2021.126896

Reference: JTEMB 126896

To appear in: *Journal of Trace Elements in Medicine and Biology*

Received Date: 16 May 2021

Revised Date: 12 September 2021

Accepted Date: 2 November 2021

Please cite this article as: Wu CX, Mao CY, Deng J, Zhang T, Zhao Y, Guan ZZ, Hu XX, Qi XL, Fluoride Induced Down-regulation of IKBKG Gene Expression Inhibits Hepatocytes Senescence, *Journal of Trace Elements in Medicine and Biology* (2021), doi: https://doi.org/10.1016/j.jtemb.2021.126896

Fluoride Induced Down-regulation of IKBKG Gene Expression Inhibits Hepatocytes Senescence

Wu CX [1, #], Mao CY[1, #], Deng J [1], Zhang T [1], Zhao Y[1], Guan ZZ [1], Hu XX [3, *], Qi XL [1, 2 *]

[1] Key Laboratory of Endemic and Minority Disease, Ministry of Education/Key Laboratory of Molecular Biology, Guizhou Medical University, Guiyang, 550004, P. R. China

[2] Translational Medicine Research Center, Guizhou Medical University, Guiyang, 550004, P. R. China

[3] School of Basic Medicine, Guizhou Medical University, Guiyang, 550004, P. R. China

***Corresponding authors:** Xiao-Lan Qi, E-mail: xiaolan76@163.com.

Xiao-Xia Hu, E-mail: 251982143@qq.com

# These authors contributed equally to this work.

ABSTRACT

Background: Accumulating evidences have confirmed that liver is one of the more severely damaged organs during chronic fluorosis. However, the detail mechanism is

unclear to data. At present, the objective of this study was to investigate the relationship between down-regulation of IKBKG gene expression and hepatocyte senescence induced by sodium fluoride (NaF).

Methods: Chronic fluorosis rats and NaF-exposure human liver L02 cells were reproduced the model of hepatocyte senescence in vivo and in vitro. The mRNA and protein levels of p16, p21 and IKBKG, the IL-8 level were determined. The role of IKBKG in fluoride-induced senescence of hepatocytes was explored by knock down in hepatocytes in vivo and in vitro.

Results: The number of senescence-positive cells in rat liver tissues was increased as well as the level of IL-8 and the expression levels of p16, p21 and IKBKG in fluoride exposure to rat depending on the fluoride concentration. The similar results were obtained in NaF treated liver L02 cells, and the number of cells that stagnated in the G2 phase increased significantly. Further, our results confirmed that decreasing the expression of IKBKG in hepatocytes could reduce fluoride-induced hepatocyte senescence and the changes of senescence-related indicators both *in vivo* and *in vitro*.

Conclusion: These results indicated that the elevated expression of IKBKG was positive relation with the fluoride-induced senescence in hepatocytes, suggesting the hepatocyte senescence might have a special relationship with fluoride-caused liver damage. Because of the present results limitation, the mechanism of fluoride induced senescence in hepatocytes should be concentrated in the future in detail, especially the novel targets for fluoride induced liver injury.

Keywords: fluorosis; IKBKG; cell senescence; hepatocyte

1. Introduction

Fluoride is a trace element with a very narrow safety threshold. Low-dose fluoride (<1 mg/L) intake is beneficial for normal bone and tooth development. However, prolonged exposure to high fluoride results in chronic fluorosis and damage to multiple tissues of the body [1]. In addition to causing skeletal fluorosis and dental fluorosis, fluoride can also induce extensive damage on soft and mineralized tissues [2, 3]. Fluorosis is a major public health issue in numerous areas around the world, including China, India, Bangladesh, South Africa, Mexico, and Argentina [4]. The pathogenesis of fluorosis is still not well understood, which hinders the prevention and treatment of fluorosis.

Cellular senescence refers to the occurrence of cell growth inhibition and the potential failure of proliferation under the act of certain physical or chemical factors, causing irreversible changes in the phenotype, structure and function of cells [5]. Senescent cells still maintain metabolic activities for a period of time, but lose their response to mitogens and the ability to synthesize DNA [6]. The stagnation of cell cycle, shortening telomeres, invaginated nuclear membranes, deformed organelles, lipofuscin deposits and other morphological changes characterize the cellular senescence, together with the expression of high enzyme activity senescence-associated β-Galactosidase (SA-β-Gal) [7]. In addition, senescence-associated secretory phenotypes (SASP) can also be secreted by senescent cells such as IL-6, IL-8, pro-inflammatory microenvironment reactive cytokines and proteases [8]. SASP further deteriorates neighboring cells, causing chronic inflammation, metabolic

disorders, and cell dysfunction. The mechanism of cellular senescence are not yet fully understood. Of note, oxidative stress is currently the more widely accepted main external cause of cell senescence [9].

Liver is one of the more severely damaged organs during chronic fluorosis. Epidemiological investigations and in vivo studies have shown that fluorosis can interfere with liver function [10]. Many studies have shown that fluoride can induce increased oxidative stress in rat liver cells, increased ROS production, mitochondrial free radical scavenging system obstacles, and significant changes in mitochondrial morphology and function [11, 12]. In addition, fluoride can directly covalently bind to DNA and cause liver DNA damage [13]. In NaF treatment of liver L02 cells, the DNA damage rate was positively correlated with the fluoride concentration [14]. The presented results showed that fluoride-induced oxidative stress and DNA damage play an important part in the pathogenesis of fluorosis. These studies suggested that fluorosis might cause liver damage by inducing cell senescence.

Researches have shown that DNA damage can stimulate the secretion of inflammatory mediators and NF-κB signaling, which consequently regulates several host defense functions related to cellular senescence [15]. Inhibitor of nuclear factor kappa B kinase subunit gamma (IKKγ, IKBKG) protein is the regulatory subunit of IκB kinase (IKK) complex and thus an essential modulator of NF-κB signaling. Recent studies have revealed that IKBKG protein has a major role in the activation process of NF-κB signaling evoked by DNA damage, which indicates that IKBKG may participate in the process of cell senescence [16]. In addition to IKK components,

IKBKG can interact with several other proteins associated with NF-κB signaling, e.g. Ataxia Telangiectasia Mutated (ATM), ELKS, receptor interacting protein1 (RIP1) and TGFβ-activated kinase1 (TAK1) [17].

In the present study, chronic fluorosis rats and human hepatic cell lines (L02) treated with sodium fluoride (NaF) were chosen as the research subjects to investigate whether NaF could induce cell senescence of hepatocytes, and the effects of IKBKG on hepatocytic senescence induced by fluoride. It may shed light on the pathogenesis of fluoride-induced liver injury.

2. Materials and Methods

2.1 Materials

Mouse anti P16 (sc-377412) and P21 (sc-6246) antibodies were purchased from Santa Cruz Biotechnology Inc, USA; rabbit anti IKBKG antibody (18474-1-AP) was purchased from Proteintech Group, Inc, USA; rabbit anti-β-actin antibody (GTX109639) was purchased from Gene Tex, USA; HRP-labeled anti-mouse secondary antibody (#7076) and anti-rabbit secondary antibody (#7074) were purchased from Cell Signaling Technology, USA.

Other reagents used in the study were as follows: NuPAGE LDS Sample Buffer (4X), NuPAGE Sample Reducing Agent (10X), NuPAGE Novex 4-12% Bis-Tris Precast, MES SDS Electrophoresis were bought from Life Technologies Corporation, USA; DMEM high glucose medium was purchased from Thermo, USA; primers for amplification of IKBKG, p16, p21 and β-actin mRNA were synthesized by Shanghai Genecore Bio Technologies, Shanghai, China; human cytokine ELISA kit IL-8 was purchased from Novus Biologicals, USA; rat ELISA kit IL-8 was purchased from Solarbio, China. Dimethyl Sulfoxide (DMSO) and other chemicals used were purchased from Sigma. The adeno-associated virus that silences the rat IKBKG gene

(named AAV-IKBKG, and the negative AAV named AAV-Neg) and RNA interference plasmid for human IKBKG gene (named plasmid sh-IKBKG and the negative control named Plasmid negative) were constructed by Shanghai Jikai Gene Company, China. The interference RNA fragment of rat IKBKG was 5' GCCAGCAATGCTACATCTT 3' and 5'CCAAGAATACGACAACCACAT3' for L02 cell IKBKG RNAi.

2.2 Experimental animals and treatment

SD (Sprague-Dawley) rats (weighing 90-120 g) were purchased from the Experimental Animal Center in Guizhou Medical University, and ethical permission for the experiment was approved by the ethical committee for experimental animal of Guizhou medical University. The humidity ranged from 30 to 55% and temperature remained between 22 and 25°C. The rats were acclimatized for one week in a housing facility before treatment.

60 SD rats were randomly divided into 6 groups with 10 rats in each group (equal number in both genders) with body weight as following: NC group (normal control group): drinking water containing less than 0.5 mg/L fluoride, low fluoride group (Low group): drinking water containing 5 mg/L fluoride, medium fluoride group (Medium group): drinking water containing 10 mg/L fluoride and high fluoride group (High group): drinking water containing 50 mg/L fluoride, High fluoride+Neg group (High+Neg group): drinking water containing 50 mg/L fluoride and tail vein injection with AAV-neg, High fluoride+AAV group (High+AAV group): drinking water containing 50 mg/L fluoride and tail vein injection with AAV-IKBKG. For the rats of High +Neg and High +AAV groups were injected with AAV-IKBKG by tail vein after feeding with NaF for 6 months and examined 4 weeks after virus injection.

2.3 L02 cell culture and treatment

L02 cells, a normal human liver cell line purchased from the cell bank of Chinese

Academy of Sciences Shanghai Branch, were grown in DMEM medium supplemented with 15 % heat-inactivated fetal bovine serum and 25 units of penicillin-streptomycin/ml, and cultured at 37 °C with 5% CO2. Concerning the effects of NaF on cell senescence, cells were divided into four groups, e.g. NC group, low NaF group (cells treated with 1 mmol/L NaF for 48h), medium NaF group (cells treated with 4 mmol/L NaF for 48h) and high NaF group (cells treated with 7 mmol/L NaF for 48h).

As for the effects of IKBKG gene knockdown on L02 cell senescence induced by fluoride, the cells were treated with 7 mmol/L NaF for 48h and then transfected with plasmid sh-IKBKG for 48h.

2.4 Analyzing the concentrations of fluoride in blood and urine by fluoride ion selective electrode method

After the rats were fed with NaF for 6 months, the urine was collected from each group for 24 hours and the rat serum was collected. The fluoride concentrations were determined by an electronic meter (PHSF-4F) and a fluoride-specific ion electrode [18]. The detection limit of F-selected electrode (PF-202-CF, INESA, Shanghai) was 0.01 mg/L. During the measurement, samples were diluted in TISAB II, a total ionic strength adjustment buffer, to adjust the pH and ionic strength of standards and urine or blood samples. The concentration was quantified against a fluoride calibration curve in a range of 0.1 to 20 mg/L prepared with a reagent blank. The measurement accuracy of ion selective electrode ranged from 97.3% to 101.9% relative to the standard fluoride solution, with the measurement errors less than ± 5%, and the recovery rate from 93.4% to 108.3%.

2.5 SA-β-gal activity Histochemical Staining to detect the L02 cell senescence and liver cell senescence of chronic fluorosis rats

After treatment, the frozen section of liver and L02 cells were rinsed with PBS and fixed for 5 min in 3% formaldehyde. SA-β-gal staining was determined using a Senescence β-galactosidase staining kit (Cell Signaling Technology, Danvers, MA, USA). 3 slides of liver tissue of each rat were analyzed, and for L02 cell assays, each experiment has three replicates, and repeated three times.

Randomly selected ten 200-fold fields of view for each cell slide, counted the number of blue-stained senescence cells under light microscope. Then the average value was used to calculate the proportion of senescence-positive cells in the total number of cells to yield the percentage of senescence-positive cells. Observing the integrated optical density (IOD) of positive-stained cells in liver tissue according to the kit instructions of SA-β-gal.

2.6 Analyzing the mRNA levels of p16, p21 and IKBKG by RT-qPCR.

The mRNA levels of p16, p21 and β-actin were determined by RT-qPCR as described previously [19]. Briefly, 2 μg of total RNA from liver of each rat were reverse transcribed to cDNA by using oligo-dT strategy. RT-qPCR was conducted on an ABI 7300 Real-time system and analyzed with the Applied Biosystems SDS2.1 software. Amplifications were performed with the universal TaqMan 2×PCR SYBR Green I Master mix according to the manufacturer's instruction. Reactions were carried out in 25-μl volume with 2.5 μl cDNA and 1.25 μl each primer to analyze the relative level of each protein (primer sequences were listed in table.1). SDS2.1 software was used for analyzing the $^{\triangle\triangle}$Ct and relative quantity (RQ) value ($RQ=2^{-\triangle\triangle}$ Ct) of each gene. The relative levels of p16 and p21gene mRNA were calculated with β-actin as an internal control.

Table.1 The primers for analyzing the mRNA levels of p16, p21 and β-actin by RT-qPCR

gene	Primer sequences (5'→3')	Amplicon size (bp)

β-actin (H)	gtgctatgttgctctagacttcg	174
	atgccacaggattccatacc	
β-actin (R)	ctttgcccagcatcaca	142
	aagcagcatttcgtcttga	
IKBKG (H)	ggccaaacaggaggtgat	153
	Ttcttctcggccagcttc	
IKBKG (R)	ttgaggatatgaggaagcg	82
	gccaaatgaaaggagtgg	
P16 (H)	gtgggcatttcttgcga	132
	tttggttctgccatttgct	
P16 (R)	gtgcggtatttgcggtatc	175
	gcgttgccagaagtgaag	
P21 (H)	atgagttgggaggaggca	111
	ctgagcgaggcacaagg	
P21 (R)	Cctcccagcctccaaactta	164
	cgccaggatcagaaacacag	

2.7 Analyzing protein levels of p16, p21 and IKBKG by Western blot.

The levels of p16, p21 and IKBKG proteins in liver tissue lysates and treated L02 cells were quantified by Western blot as described previously [19]. In sum, proteins extracted from liver tissues or cells were quantitated by BCA Assay. The proteins were separated with 10% SDS-PAG electrophoresis, transferred to polyvinylidene difluoride membranes and blocked with 5% skimmed milk for 2h at room temperature (RT). Then, the membranes were incubated with primary antibodies (against p16, p21 or IKBKG) overnight at 4 ℃. After rinsing, secondary antibody conjugated with HRP was added to the membranes and incubated for 1 h at RT. Finally, the protein blots were detected with chemiluminescence substrate (ECL) and exposed to film.

After stripping the antibodies off the membranes, they were incubated again with

primary mouse antibody against β-actin (1:5000) for 120 min and then incubated with HRP-conjugated anti-mouse IgG for 60 min at RT. ImageJ software was used to analyze the intensity of each protein bands, and β-actin band was used as internal control to calculate the relative expression levels of the proteins.

2.8 Analyzing the level of IL-8 by ELISA method

The levels of IL-8 in liver tissue lysates and culture media from L02 cells treated with NaF were determined by ELISA according to the protocol. The liver tissue was homogenated with a tissue grinder, centrifuged, and supernatant was collected. The culture media were collected after 48 hrs of exposure and then centrifuged. All samples were stored at -80 °C for subsequent analysis. The OD was measured at 450 nm with a microplate ELISA reader (Bio-Rad).

2.9 Analyzing the cell cycle by flow cytometry

The cells were collected and rinsed with PBS for 3 times, then cells were fixed with pre-chilled 70% ethanol for at least 2 hours at -20°C. Centrifuge fixed cells was decanted with supernatant (ethanol) and rinsed once with 1x PBS to remove ethanol and then 300 μL of PI staining solution per sample was added (composed of 140 μM PI, 38 mM sodium citrate, 10μg/mL RNase A and 0.01%Triton X-100), samples were mixed and incubated for 30 min in darkness at 37 °C. Then the cell cycle was measured by flow cytometry.

2.10 Statistical analysis

All data was presented as means ±SD. The values were examined using two-tail Student's t-test, and one-way ANOVA with SPSS 22 software (USA), differences between means were considered statistically significant when $p < 0.05$.

3. Results

3.1 Occurrence of dental fluorosis in rats with chronic fluorosis

After feeding water to the rats with different concentrations of NaF for 6 months, it was found that the teeth of control group were normal; in the low-fluoride group, the incidence of mild dental fluorosis was 30%, and the moderate dental fluorosis rate was 20%; as for rats in the medium fluoride group, the incidence of mild dental fluorosis was 40%, and the moderate dental fluorosis rate was 60%; as for rats in the high fluoride group, the incidence of mild dental fluorosis was 10%, the moderate dental fluorosis rate was 50%, and the severe dental fluorosis rate was 30%.

3.2 Fluoride ion content in urine and blood of rats with chronic fluorosis

The results showed that the fluoride ion content in urine and blood of rats respectively fed with 5 mg/L, 20 mg/L, and 50 mg/L fluoride water increased gradually. Compared with the normal control group, the difference was statistically significant. (Table.2).

Table 2 Fluoride ion content in urine and blood of rats with chronic fluorosis ($\bar{x}\pm s$)

Group	Urine (mg/L)	Blood (mg/L)
WT	1.40±0.21	0.02±0.001
Low	4.10±0.37**	0.05±0.005**
Medium	6.57±0.33**	0.08±0.012**
High	14.26±2.11**	0.13±0.017**

The values were shown as mean ± SD of each independent experiment (n=10). **<0.01 as compared to WT group.

3.3 Results of SA-β-gal staining in liver of fluorosis rats

When the cells are senescent, the senescent cells are blue after staining with β-galactosidase. The experimental results showed that a small number of senescent cells in the liver of the normal control group were stained blue (Figure 1A). With the

increase of fluoride concentration, the area of rat liver tissue stained blue gradually increased (Figure 1B-D) compared with the normal control group, the difference was statistically significant (P<0.01) (Figure 1E).

After fluorosis rats were injected with AAV-IKBKG through the tail vein, compared with the high fluorosis group (Fig. 2A), senescence-positive cells in the liver significantly decreased (Fig. 2C), and the difference was statistically significant (Fig. 2D).

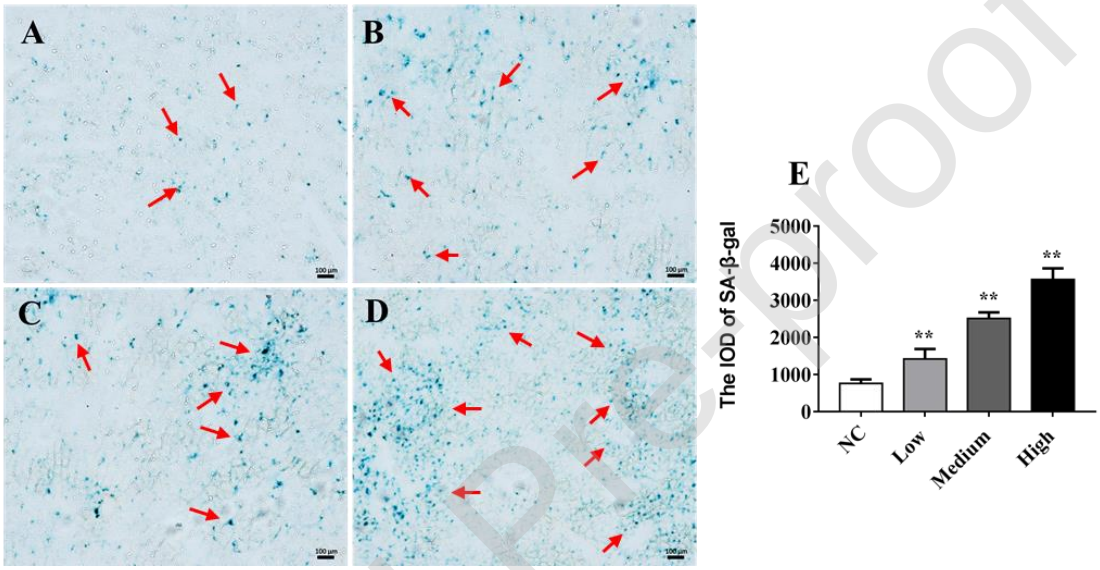

Fig 1. Results of SA-β-gal staining in liver of fluorosis rats

A: NC: normal control group, B: Low: low fluoride group, C: Medium: medium fluoride group, D: High: high fluoride group, E: the IOD of SA-β- gal staining. The magnification of the microscope was 100 times, scale bar was indicated in each picture. As compared to NC group (A), the SA-β-gal (blue) positive cells gradually increased significantly with the increase of NaF concentration (B-D). Data were presented as means ± SD (n=10). **P<0.01 vs. Control group.

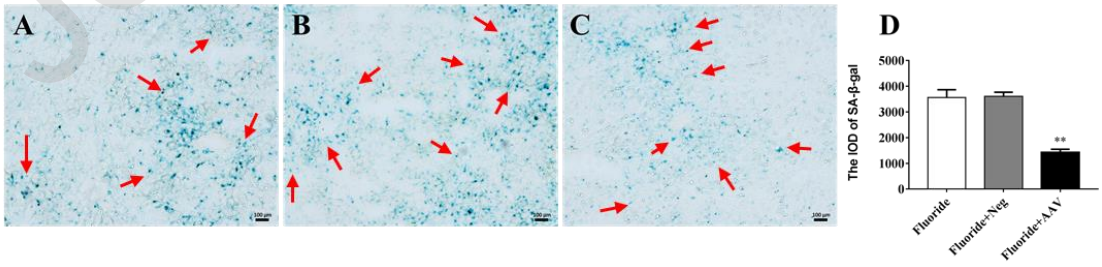

Fig 2. Results of SA-β-gal staining in liver of fluorosis rats with AAV-IKBKG injection by tail

vein

A: Fluoride: high fluoride group, B: Fluoride+Neg: high fluoride group injected with AAV-Neg by tail vein, C: Fluoride+AAV: high fluoride group injected with AAV-IKBKG, D: the IOD of SA-β- gal staining. The magnification of the microscope was 100 times, scale bar was indicated in each picture. As compared to fluoride group (A), the SA-β-gal (blue) positive cells were decreased significantly (C). Data were presented as means ± SD (n=10). ** P<0.01 vs. Fluoride group.

3.4 Levels of P16, P21, and IKBKG mRNA and protein in the liver tissue of fluorosis rats

Levels of IKBKG mRNA (Fig. 3A), P16 mRNA (Fig. 3C), P21 mRNA (Fig. 3E) and protein (Fig. 3B, 3D, 3F) were increased in the rats of medium and high fluoride groups compared to those in the control group, while there was no difference of P16 mRNA and protein level in the low fluoride group compared to that of control. With the degree of fluorosis increase, the levels of IKBKG, P16 and P21mRNA and protein were increased significantly.

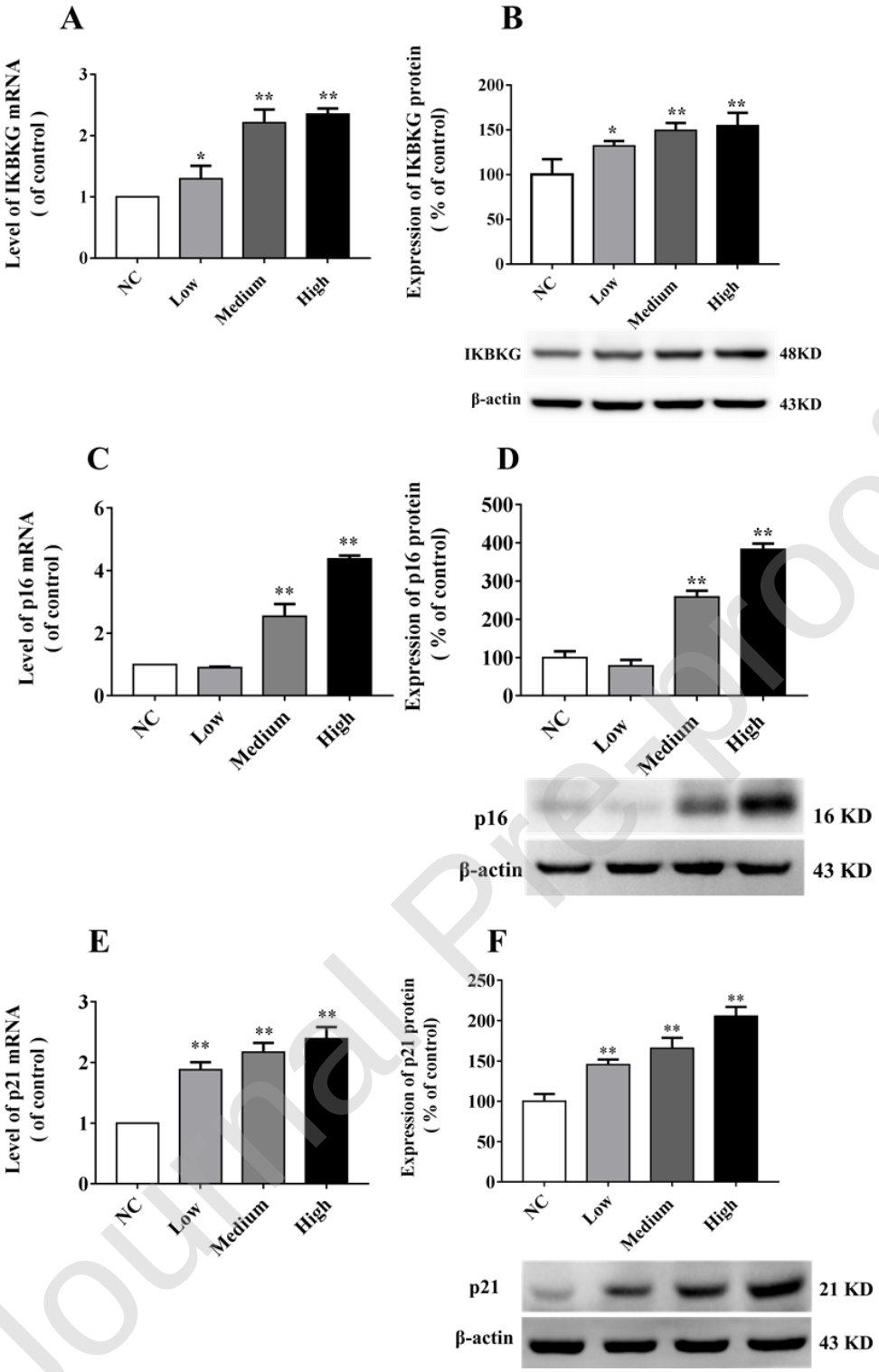

Fig. 3 The mRNA and protein levels of IKBKG (A, B), P16 (D, D) and P21 (E, F) in the liver tissue of fluorosis rats. The mRNA and protein levels, as well as those for β-actin (as an internal standard), were determined by real time RT-PCR and Western blotting respectively, and the values were shown as means ± SD (n=10). ** $P < 0.01$ in comparison to the corresponding control value.

Interestingly, when fluorosis rats were injected with AAV-IKBKG through the tail vein, compared with the high fluorosis group, the mRNA and protein levels of IKBKG (Fig.4), P16 (Fig. 5A and B) and P21 (Fig. 5C and D) were decreased significantly.

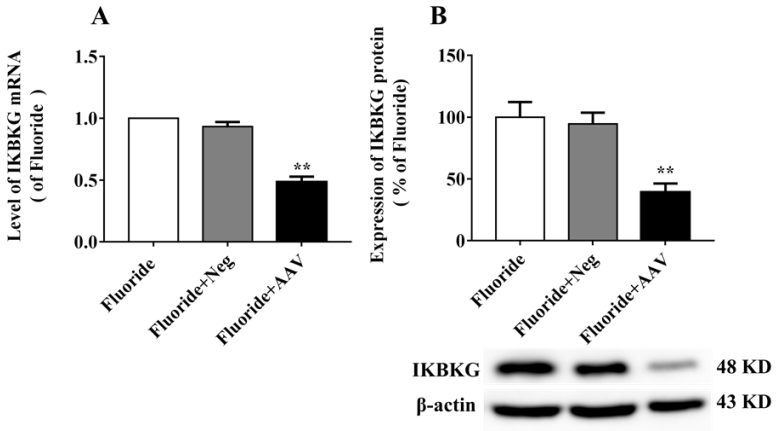

Fig. 4 The mRNA (A) and protein (B) levels of IKBKG in the liver tissue of fluorosis rats injected with AAV-IKBKG. The mRNA and protein levels, as well as those for β-actin (as an internal standard), were determined by real time RT-PCR and Western blotting respectively, and the values were shown as means ± SD (n=10). ** $P < 0.01$ in comparison to the corresponding control value.

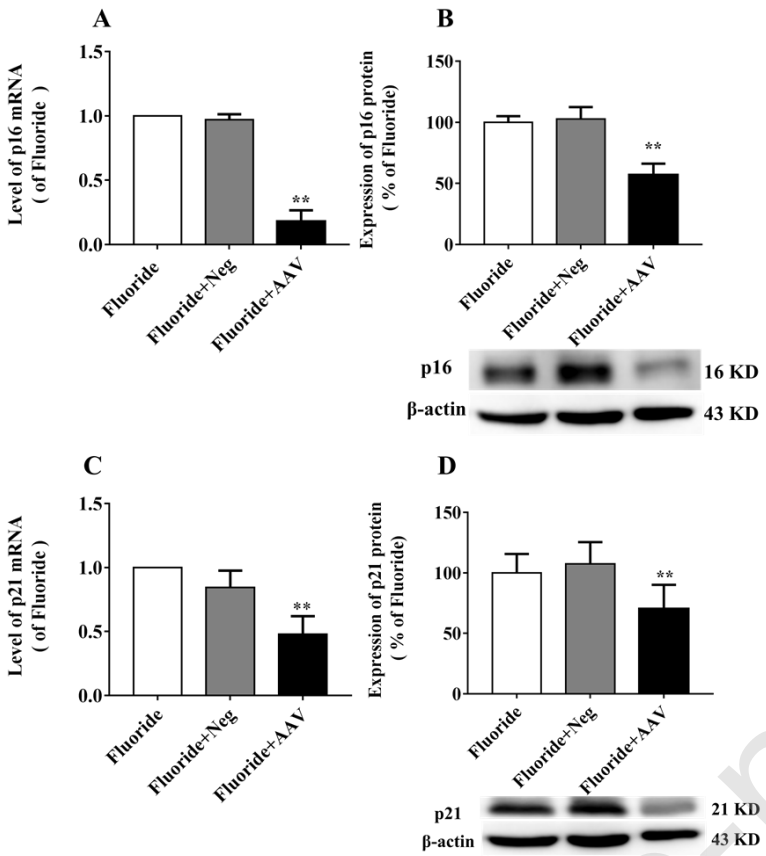

Fig. 5 The mRNA and protein levels of P16 (A, B) and P21 (C, D) in the liver tissue of fluorosis rats injected with AAV-IKBKG. The mRNA and protein levels, as well as those for β-actin (as an internal standard), were determined by real time RT-PCR and Western blotting respectively, and the values were shown as means ± SD (n=10). ** $P < 0.01$ in comparison to the corresponding control value.

3.5 Level of IL-8 in liver tissue of fluorosis rats

ELISA results showed that with the increase of fluoride concentration, the level of IL-8 gradually increased, and compared with the normal control group, the difference was statistically significant (Table. 3). While the IL-8 level decreased significantly in the liver of high fluoride treated rats injected with AAV-IKBKG compared with that of high fluoride group.

Table 3 Expression level of IL-8 in liver homogenate of rats in each group ($\bar{x}\pm s$)

Group	Expression level of IL-8 (pg/mL)
NC	717.09±110.36
Low	1142.09±118.08**
Medium	1210.98±177.09**
High	1228.47±112.67**
Fluoride+Neg	1189.25±145.77**
Fluoride+AAV	764.25±123.16##

Data was presented as means ± SD of each independent experiment (n=10). **P<0.01 vs. Normal Control group. ## P<0.01 vs. High fluoride group

3.6 Results of SA-β-gal staining in liver L02 cells treated with NaF

After treating L02 cells with different concentrations of NaF for 48 h, the results of SA-β-gal staining showed that the number of senescence-positive cells increased significantly (blue cells) with the increase of NaF concentration (Figure 6B-D). Compared with the control group, the difference was statistically significant (Figure 6E).

When L02 cells were exposed to 7mmol/L NaF and transfected with IKBKG-shRNA to decrease the expression of IKBKG, the senescence-positive cells in L02 cells were reduced compared with L02 cells treated with 7mmol/L NaF (Fig. 7).

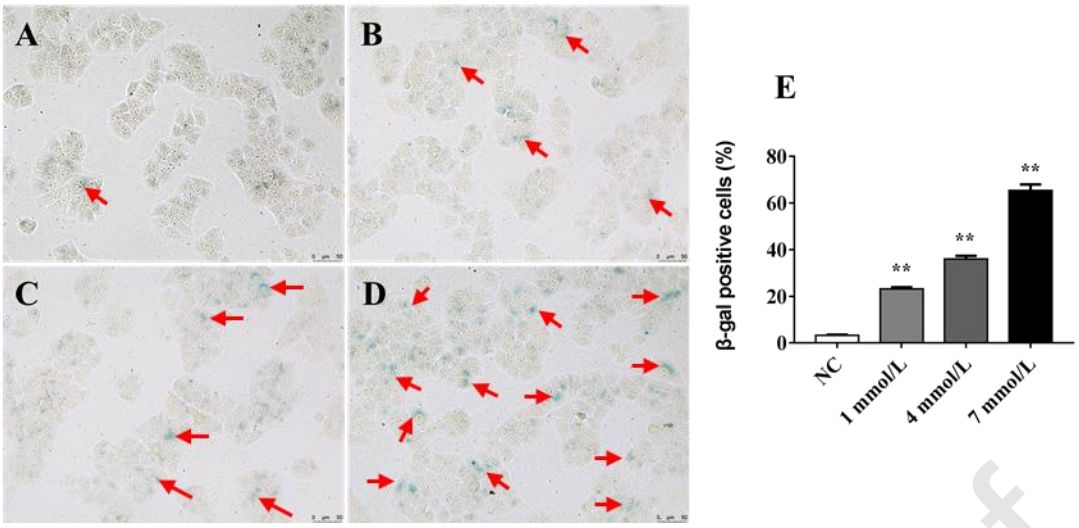

Fig. 6 SA-β-gal positive cells in L02 cells treated with NaF

A. NC: normal control group, B. 1 mmol/L: L02 cells treated with 1mmol/L NaF, C. 4mmol/L: L02 cells treated with 4 mmol/L NaF, D. 7mmol/L: L02 cells treated with 7 mmol/L NaF, E. β-gal positive cells in each group. The magnification of the microscope was 200 times, scale bar was indicated in each picture. As compared to NC group (A), the β-gal positive cells were gradually increased significantly with the increase of NaF treated (B-D). Data was presented as means ± SD (n=9). **P<0.01 vs. NC group.

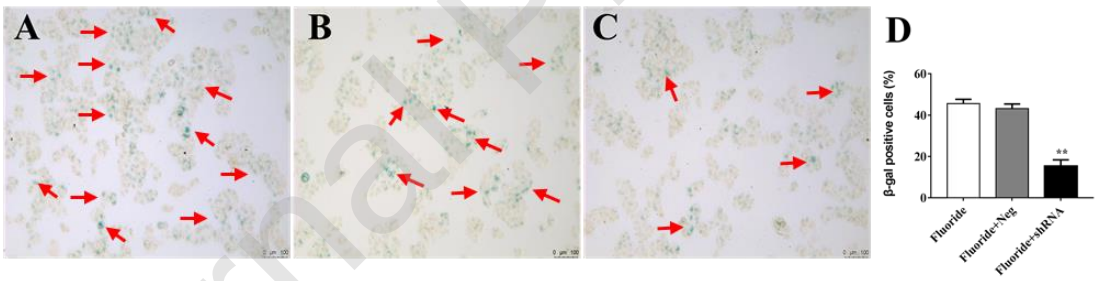

Fig. 7. Results of SA-β-gal staining in NaF treated L02 cells transfected with sh-IKBKG

A. Fluoride: L02 cells treated with 7 mmol/L NaF, B. Fluoride+Neg: L02 cells treated with 7 mmol/L NaF and transfected with sh-Neg, C. Fluoride+shRNA: L02 cells treated with 7 mmol/L NaF and transfected with sh-IKBKG, D. β-gal positive cells in each group. The magnification of the microscope was 200 times, scale bar was indicated in each picture. As compared to fluoride group (A), the β-gal (blue) positive cells were decreased significantly (C). Data was presented as the means ± SD (n=9). ** P<0.01 vs. Fluoride group.

3.7 mRNA and protein levels of P16, P21, and IKBKG in L02 cells treated with NaF

The levels of IKBKG mRNA (Fig. 8A), P16 mRNA (Fig. 8C), P21 mRNA (Fig. 8E) and protein (Fig. 8B, 8D,8F) levels were increased in L02 cells treated with different concentrations of NaF. As the concentration of sodium fluoride increased, the mRNA and protein levels of IKBKG, P16 and P21 gradually increased in a dose-dependent manner. When L02 cells exposed to 7mmol/L NaF were transfected with sh-IKBKG, the expression level of IKBKG was decreased (Fig.9), and compared with the high NaF treated group, the mRNA and protein levels of P16 (Fig. 10A and B) and P21 (Fig. 10C and D) were decreased significantly.

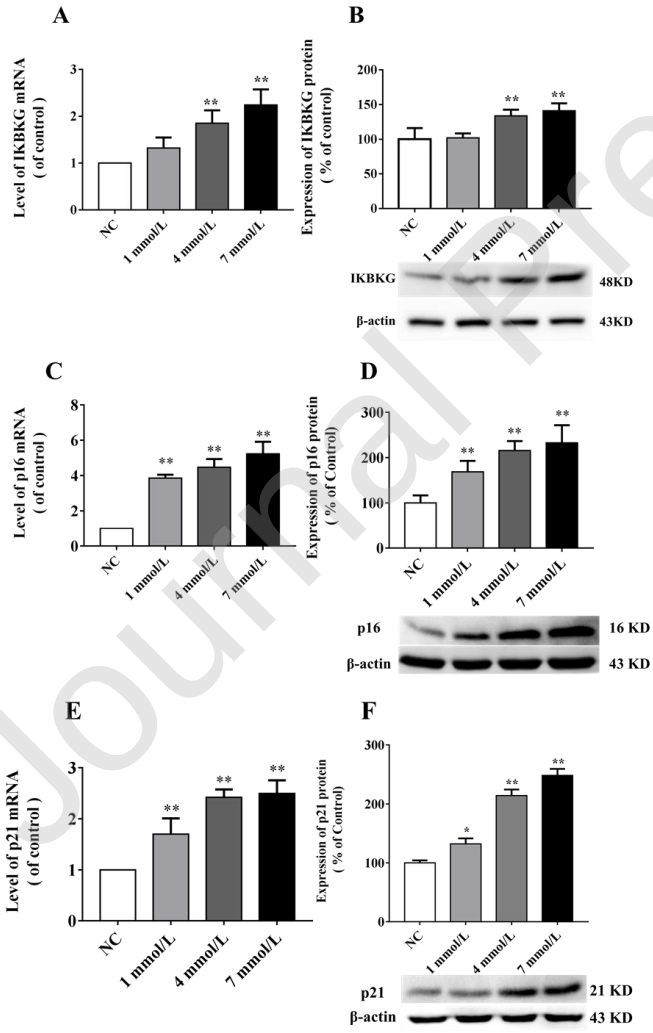

Fig.8 mRNA and protein levels of IKBKG (A, B), P16 (C, D) and P21 (E, F) in L02 cells

treated with NaF. mRNA and protein levels, as well as those for β-actin (as an internal standard), were determined by real time RT-PCR and Western blotting respectively, and the values were shown as means ± SD (n=9). ** $P < 0.01$ in comparison to the corresponding control value.

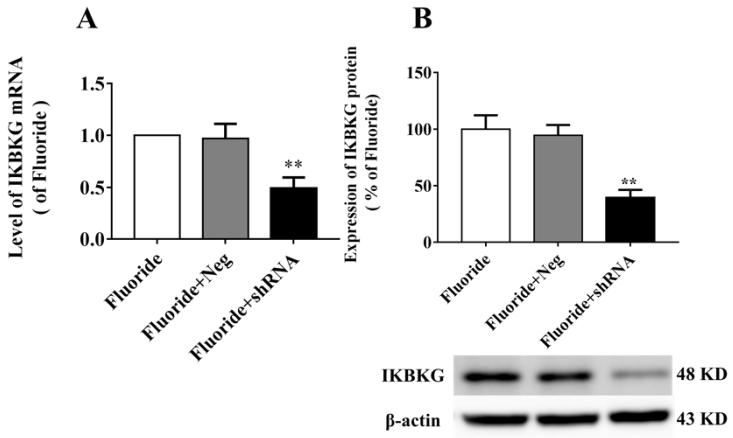

Fig.9. mRNA and protein levels of IKBKG in L02 cells exposed to 7mmol/L NaF and transfected with sh-IKBKG. mRNA and protein levels, as well as those for β-actin (as an internal standard), were determined by real time RT-PCR and Western blotting respectively, and the values were shown as means ± SD (n=9). ** $P < 0.01$ in comparison to the corresponding control value.

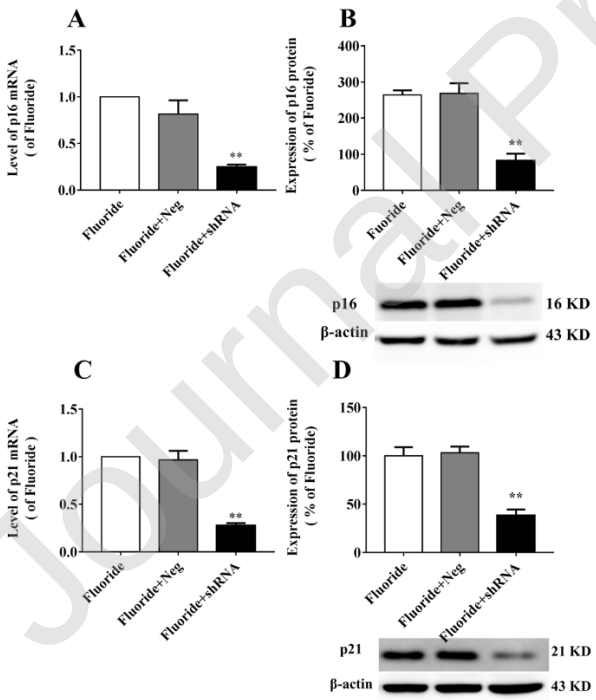

Fig.10. mRNA and protein levels of P16 (A, B) and P21 (C, D) in L02 cells exposed to 7mmol/L NaF and transfected with sh-IKBKG. The mRNA and protein levels, as well as those for β-actin (as an internal standard), were determined by real time RT-PCR and Western blotting

respectively, and the values were shown as means ± SD (n=9). ** $P < 0.01$ in comparison to the corresponding control value.

3.8 Level of IL-8 in L02 cells treated with NaF and transfected with sh-IKBKG

ELISA results showed that with the increase of NaF concentration, the level of IL-8 gradually increased; compared with the normal control group, the difference was statistically significant (Table. 4). IL-8 level decreased significantly in L02 cells exposed to 7mmol/L NaF and transfected with sh-IKBKG compared with Fluoride+NC group.

Table 4 Expression level of IL-8 in L02 cells treated with different concentrations of NaF and transfected with sh-IKBKG

Groups	IL-8 (pg/mL)
NC	76.31±3.77
low NaF group	84.46±1.73**
middle NaF group	90.75±6.56**
High NaF group	98.70±4.50**
Fluoride+NC	509.59±51.66
Fluoride+shRNA	290.86±61.86 ##

Data was presented as means ± SD of each independent experiment (n=10). **P<0.01 vs. Normal Control group. ## P<0.01 vs. Fluoride + NC group

3.9 Cell cycle of L02 cells treated with 7mmol/L NaF and transfected with sh-IKBKG

Cell cycle detection by flow cytometry showed that compared with normal control group, the cell cycle of L02 treated with different concentrations of NaF mainly stagnated in the G2 phase in a dose-dependent manner (Fig. 11). After transfection of IKBKG-shRNA, the number of L02 cells in the G2 phase was significantly reduced compared with the L02 cell group treated with high fluoride concentration (Fig. 11).

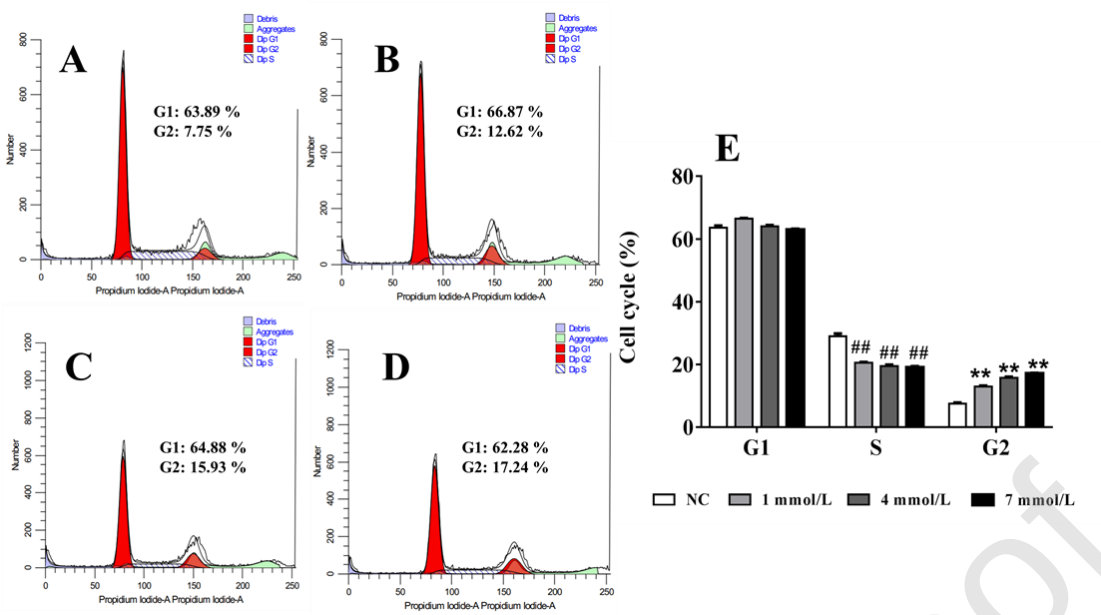

Fig. 11 Cell cycle of L02 cells treated with different concentration of NaF.

A. NC group, B. Low NaF group (Low): L02 cells treated with 1mmol/L NaF, C. Medium NaF group (Medium): L02 cells treated with 4mmol/L NaF, D. High NaF group (High): L02 cells treated with 7 mmol/L NaF, E. cell cycle of each group. The cell cycle of L02 cells in each group was determined by cell cytometry, and the values were shown as means ± SD (n=9). ## and ** P < 0.01 in comparison to the corresponding control value.

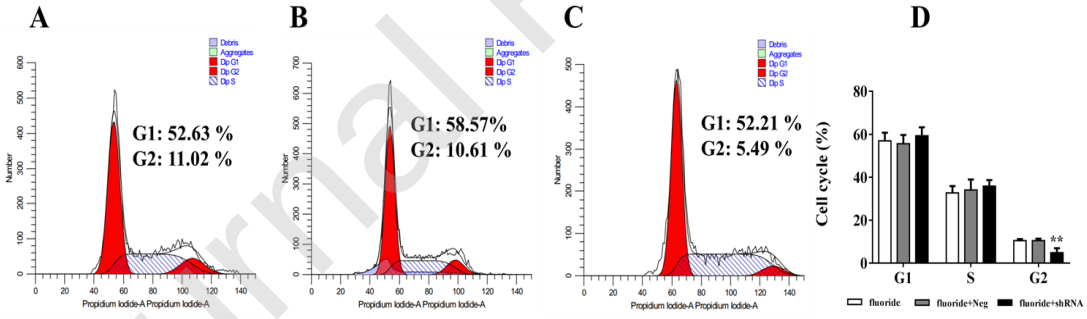

Fig. 12 Cell cycle of L02 cells treated with 7 mmol/L NaF and transfected with sh-IKBKG.

A. Fluoride: L02 cells treated with 7 mmol/L NaF, B. Fluoride+Neg: L02 cells treated with 7 mmol/L NaF and transfected with sh-Neg, C. Fluoride+shRNA: L02 cells treated with 7 mmol/L NaF and transfected with sh-IKBKG, D. cell cycle of L02 cells in each group. The cell cycle of L02 cells in each group was determined by cell cytometry, and the values were shown as means ± SD (n=9). ** P<0.01 vs. Fluoride group.

4. Discussion

Cellular senescence is a pathophysiological phase in which the cell cycle is arrested and cells stop growing. In recent years, cellular senescence has been widely highlighted as one of the pathogenesis mechanisms that regulate various diseases such as tumors, degenerative diseases, and chronic diseases [20]. The reason and mechanism of cell senescence are not fully understood. Oxidative stress is the main external cause of cell senescence that is more generally accepted. Cells undergoing senescence have characteristic features, displaying a large and flat morphology: an increase in SA-β-gal, DNA damage, and a stable cell cycle arrest executed by interplaying between the RB and p53 tumor suppressor pathways (often accumulate the $p16^{INK4a}$, $p15^{INK4b}$, and $p21^{Cip1/Waf1}$ cyclin-dependent kinase inhibitors that engage the RB pathway or mediate p53 effects accordingly) [21, 22]. Previous studies have shown that there are senescent cells in the liver of patients with non-alcoholic fatty liver (NAFLD) and cirrhosis. The increase in the number of senescent cells can promote the occurrence of NAFLD, but the underlying mechanism is not fully elucidated [23, 24].

It has been verified that the increased oxidative stress induced by fluoride was associated with DNA fragmentation in rat hepatocytes, which was one of the main mechanisms leading to liver damage. As oxidative stress is one of the main causes of cell senescence, these studies suggested that fluorosis may cause liver damage by inducing cell senescence. However, there are very few studies on the toxic effects of fluoride by inducing cell senescence. The present study investigated the effects of fluoride on hepatocyte senescence through *in vitro* and *in vivo* experiments.

The results showed that fluoride could induce cell senescence by β-galactosidase staining on frozen sections of liver tissues of chronic fluorosis rats and L02 cells

treated with different concentrations of NaF. With the increase of fluoride concentration, the SA-β-gal-positive cells were increased obviously, suggesting that the degree of senescence was positively correlated with the concentration of fluoride. Concerning the levels of p16 and p21, the hallmarks of cell senescence, it was found that the expression levels of p16 and p21 were increased in a concentration-dependent manner in fluorosis rats' liver and NaF treated L02 cells, which further confirmed that fluoride could induce hepatocyte senescence. As p16 was the main tumor suppressor, which could induce cell senescence and cycle arrest. After exposure NaF to L02 cell, the cell cycle was arrested in the G2 phase by flow cytometry. At the same time, the level of IL-8 in the liver tissue of fluorosis rats and culture medium of fluoride-treated L02 cells were significantly increased. Taken together, our results confirmed that fluoride could induce hepatocyte senescence, which might play an important role in the fluoride induced liver damage.

It is clear now that SASP components actively participate in the senescence process. For example, key SASP factors (IL-6 and IL-8) act in an autocrine feedback loop to reinforce the senescence growth arrest. Nuclear factor-κB (NF-κB) is a master regulator of SASP and is used to further probe the impact of SASP biology on the senescence program [25]. A large number of studies suggested that NF-κB signaling was highly activated in cellular senescence [15]. NF-κB gene expression was also enhanced in primary rat hippocampal neurons by fluoride treatment in a dose-dependent manner, which meant fluoride might regulate cell senescence by activating NF-κB signaling [26]. The NF-κB system is an evolutionarily conserved signaling pathway, which can be triggered by not only immune activation but also diverse external/internal danger signals associated with senescence and even the aging process (oxidative and genotoxic stresses). IKBKG is generally called NEMO, an

important regulatory component of IKK complex linked upstream to genotoxic signals and IL-1 and TNF receptor mediated signaling [16]. Recent studies have shown that IKBKG protein plays a major role in the activation of NF-κB signals caused by DNA damage, which suggests that IKBKG may be involved in the process of cell senescence [17, 27]. Studies have found that IKBKG can also regulate liver diseases at different functional levels [28] [29]. This study further explored the role of IKBKG in fluoride-induced hepatocyte senescence, hoping to provide a theoretical basis for the pathogenesis of fluorosis.

The results showed that the expression of IKBKG increased in liver tissues of chronic fluorosis rats and liver L02 cells exposured with NaF in a concentration-dependent manner. The results suggested that fluoride might induce hepatocyte senescence via up-regulating the expression of IKBKG. To further verify the role of IKBKG in fluoride-induced hepatocyte senescence, tail vein injection of AAV-IKBKG and transfected sh-IKBKG to L02 cells were adopted to knock down the level of IKBKG. The results showed that compared with the fluorosis rat or L02 cells treated with fluoride, the SA-β-gal-positive cells were decreased, the expression levels of P16 and P21 decreased, the IL-8 level decreased in rat liver or L02 cells treated with NaF and down-regulation of IKBKG, and the number of L02 cells arrested in the G2 phase was also reduced.

In conclusion, the chronic fluorosis rats and human L02 cells exposed with NaF as to evaluate whether fluoride could induce hepatocyte senescence and its potential regulated mechanism. The results indicated that fluoride might cause liver damage by inducing cell senescence, and its mechanism might be related to the up-regulation of IKBKG expression in hepatocytes. This research might shed more light on the underlying pathogenesis of fluorosis, the senescence is complex pathophysiological

process, IKBKG just as a pathological factors and further researches should be designed to fully elucidate the regulation signal pathway of IKBKG in the role of cell senescence in the toxicity of fluoride.

Conflict of interests

All authors declare that they have no competing interests. All authors have read and approved the final manuscript.

Author Contributions

QXL, HXX and WCX conceived and designed the research. WCX, MCY, DJ, ZT performed the experiments. QXL , WCX , ZY, GZZ wrote the manuscript. All authors have read and approved the final manuscript.

Acknowledgements

None

Funding

This work was financially supported by the Chinese National Natural Science Foundation (U1812403) and the Department of Education of Guizhou Province (KY [2021]313).

References

[1] A.P. Daiwile, S. Sivanesan, P. Tarale, P.K. Naoghare, A. Bafana, D. Parmar, K. Kannan, Role of fluoride induced histone trimethylation in development of skeletal fluorosis, Environ Toxicol Pharmacol 57 (2018) 159-165.

[2] R.W. Dharmaratne, Exploring the role of excess fluoride in chronic kidney disease: A review, Hum Exp Toxicol 38(3) (2019) 269-279.

[3] X.X. Zeng, J. Deng, J. Xiang, Y.T. Dong, K. Cao, X.H. Liu, D. Chen, L.Y. Ran, Y. Yang, Z.Z. Guan, Protections against toxicity in the brains of rat with chronic fluorosis and primary neurons

exposed to fluoride by resveratrol involves nicotinic acetylcholine receptors, J Trace Elem Med Biol 60 (2020) 126475.

[4] E. Perumal, V. Paul, V. Govindarajan, L. Panneerselvam, A brief review on experimental fluorosis, Toxicol Lett 223(2) (2013) 236-51.

[5] M.J. Regulski, Cellular Senescence: What, Why, and How, Wounds 29(6) (2017) 168-174.

[6] A. Bernadotte, V.M. Mikhelson, I.M. Spivak, Markers of cellular senescence. Telomere shortening as a marker of cellular senescence, Aging (Albany NY) 8(1) (2016) 3-11.

[7] A. Hernandez-Segura, J. Nehme, M. Demaria, Hallmarks of Cellular Senescence, Trends Cell Biol 28(6) (2018) 436-453.

[8] S. Lopes-Paciencia, E. Saint-Germain, M.C. Rowell, A.F. Ruiz, P. Kalegari, G. Ferbeyre, The senescence-associated secretory phenotype and its regulation, Cytokine 117 (2019) 15-22.

[9] J. Janikiewicz, J. Szymanski, D. Malinska, P. Patalas-Krawczyk, B. Michalska, J. Duszynski, C. Giorgi, M. Bonora, A. Dobrzyn, M.R. Wieckowski, Mitochondria-associated membranes in aging and senescence: structure, function, and dynamics, Cell Death Dis 9(3) (2018) 332.

[10] U. Efe, S. Dede, V. Yuksek, S. Cetin, Apoptotic and Oxidative Mechanisms in Liver and Kidney Tissues of Sheep with Fluorosis, Biol Trace Elem Res 199(1) (2021) 136-141.

[11] H.W. Wang, J. Liu, S.S. Wei, W.P. Zhao, S.Q. Zhu, B.H. Zhou, Mitochondrial respiratory chain damage and mitochondrial fusion disorder are involved in liver dysfunction of fluoride-induced mice, Chemosphere 241 (2020) 125099.

[12] Z. Zhang, B. Zhou, H. Wang, F. Wang, Y. Song, S. Liu, S. Xi, Maize purple plant pigment protects against fluoride-induced oxidative damage of liver and kidney in rats, Int J Environ Res Public Health 11(1) (2014) 1020-33.

[13] G.H. Song, F.B. Huang, J.P. Gao, M.L. Liu, W.B. Pang, W. Li, X.Y. Yan, M.J. Huo, X. Yang, Effects of Fluoride on DNA Damage and Caspase-Mediated Apoptosis in the Liver of Rats, Biol Trace Elem Res 166(2) (2015) 173-82.

[14] A.G. Wang, T. Xia, Q.L. Chu, M. Zhang, F. Liu, X.M. Chen, K.D. Yang, Effects of fluoride on lipid peroxidation, DNA damage and apoptosis in human embryo hepatocytes, Biomed Environ Sci 17(2) (2004) 217-22.

[15] J. Zhao, L. Zhang, A. Lu, Y. Han, D. Colangelo, C. Bukata, A. Scibetta, M.J. Yousefzadeh, X. Li, A.U. Gurkar, S.J. McGowan, L. Angelini, R. O'Kelly, H. Li, L. Corbo, T. Sano, H. Nick, E.

Pola, S.P.S. Pilla, W.C. Ladiges, N. Vo, J. Huard, L.J. Niedernhofer, P.D. Robbins, ATM is a key driver of NF-kappaB-dependent DNA-damage-induced senescence, stemcell dysfunction and aging, Aging (Albany NY) 12(6) (2020) 4688-4710.

[16] A.S. Shifera, Protein-protein interactions involving IKKgamma (NEMO) that promote the activation of NF-kappaB, J Cell Physiol 223(3) (2010) 558-61.

[17] A. Salminen, A. Kauppinen, K. Kaarniranta, Emerging role of NF-kappaB signaling in the induction of senescence-associated secretory phenotype (SASP), Cell Signal 24(4) (2012) 835-45.

[18] C.X. Wu, Y.H. Wang, Y. Li, Z.Z. Guan, X.L. Qi, Changes of DNA repair gene methylation in blood of chronic fluorosis patients and rats, J Trace Elem Med Biol 50 (2018) 223-228.

[19] X.L. Qi, K. Ou-Yang, J.M. Ren, C.X. Wu, Y. Xiao, Y. Li, Z.Z. Guan, Preventing expression of the nicotinic receptor subunit alpha7 in SH-SY5Y cells with interference RNA indicates that this receptor may protect against the neurotoxicity of Abeta, Neurochem Res 38(5) (2013) 943-50.

[20] S. He, N.E. Sharpless, Senescence in Health and Disease, Cell 169(6) (2017) 1000-1011.

[21] D.J. Baker, B.G. Childs, M. Durik, M.E. Wijers, C.J. Sieben, J. Zhong, R.A. Saltness, K.B. Jeganathan, G.C. Verzosa, A. Pezeshki, K. Khazaie, J.D. Miller, J.M. van Deursen, Naturally occurring p16(Ink4a)-positive cells shorten healthy lifespan, Nature 530(7589) (2016) 184-9.

[22] M. Pinto, A.M. Pickrell, X. Wang, S.R. Bacman, A. Yu, A. Hida, L.M. Dillon, P.D. Morton, T.R. Malek, S.L. Williams, C.T. Moraes, Transient mitochondrial DNA double strand breaks in mice cause accelerated aging phenotypes in a ROS-dependent but p53/p21-independent manner, Cell Death Differ 24(2) (2017) 288-299.

[23] M. Ogrodnik, S. Miwa, T. Tchkonia, D. Tiniakos, C.L. Wilson, A. Lahat, C.P. Day, A. Burt, A. Palmer, Q.M. Anstee, S.N. Grellscheid, J.H.J. Hoeijmakers, S. Barnhoorn, D.A. Mann, T.G. Bird, W.P. Vermeij, J.L. Kirkland, J.F. Passos, T. von Zglinicki, D. Jurk, Cellular senescence drives age-dependent hepatic steatosis, Nat Commun 8 (2017) 15691.

[24] A.M. Papatheodoridi, L. Chrysavgis, M. Koutsilieris, A. Chatzigeorgiou, The Role of Senescence in the Development of Nonalcoholic Fatty Liver Disease and Progression to Nonalcoholic Steatohepatitis, Hepatology 71(1) (2020) 363-374.

[25] Y. Chien, C. Scuoppo, X. Wang, X. Fang, B. Balgley, J.E. Bolden, P. Premsrirut, W. Luo, A. Chicas, C.S. Lee, S.C. Kogan, S.W. Lowe, Control of the senescence-associated secretory phenotype by NF-kappaB promotes senescence and enhances chemosensitivity, Genes Dev 25(20)

(2011) 2125-36.

[26] M. Zhang, A. Wang, T. Xia, P. He, Effects of fluoride on DNA damage, S-phase cell-cycle arrest and the expression of NF-kappaB in primary cultured rat hippocampal neurons, Toxicol Lett 179(1) (2008) 1-5.

[27] J. Fu, D. Huang, F. Yuan, N. Xie, Q. Li, X. Sun, X. Zhou, G. Li, T. Tong, Y. Zhang, TRAF-interacting protein with forkhead-associated domain (TIFA) transduces DNA damage-induced activation of NF-kappaB, J Biol Chem 293(19) (2018) 7268-7280.

[28] T. Luedde, N. Beraza, V. Kotsikoris, G. van Loo, A. Nenci, R. De Vos, T. Roskams, C. Trautwein, M. Pasparakis, Deletion of NEMO/IKKgamma in liver parenchymal cells causes steatohepatitis and hepatocellular carcinoma, Cancer Cell 11(2) (2007) 119-32.

[29] H. Pereira, A.S. Dionizio, T.T. Araujo, M.D.S. Fernandes, F.G. Iano, M.A.R. Buzalaf, Proposed mechanism for understanding the dose- and time-dependency of the effects of fluoride in the liver, Toxicol Appl Pharmacol 358 (2018) 68-75.